J Korean Radiol Soc 2003;49:387 - 392

Turnover in Intracranial Aneurysm Phantoms: Its Relation to Neck Size[1]

Tae-Sub Chung, M.D., Young-Jun Lee, M.D., Yoon-Chul Rhim, PhD.[2]

Purpose: To evaluate the physiologic background of aneurysms poorly visualized during 3D-TOF MRA, contrast-enhanced MRA (CEMRA) and DSA due to hemodynamic isolation.

Materials and Methods: Using handmade elastic silicon phantoms to represent terminal basilar tip aneurysms, 3D-TOF MRA, CEMRA and DSA were used to determine blood turnover. Aneurysmal neck size was 2 mm and 10 mm, and the use of a pulsatile pump also helped recreate human physiologic parameters. We compared the results with those of computational fluid dynamics.

Results: DSA images of the narrow-necked aneurysm showed that a small volume of contrast medium washed into it during the systolic phase. As the width of its neck increased, the turnover volume of fragments of contrast bolus also increased. At CEMRA, the broad-necked aneurysm was visualized as the main bolus of Gd-DTPA passed through it, and at delayed CEMRA, the narrow-necked aneurysm was visualized faintly after the passage of bolus Gd-DTPA. The results correlated closely with those of 3D-TOF MRA and computational fluid dynamics.

Conclusion: The visualization of intracranial aneurysms at 3D-TOF MRA, CEMRA and DSA was greatly dependent upon blood turnover, which varied according to aneurismal neck size. A narrow-necked aneurysm might be missed at 3D-TOF MRA, CEMRA and DSA due to hemodynamic isolation.

Index words : Aneurysm, cerebral
Magnetic resonance (MR), vascular studies
Magnetic resonance (MR), experimental
Digital subtraction angiography

[1]Department of Diagnostic Radiology and the Research Institute of Radiological Science (T.-S.C., Y.-J.L.), Brain Korea 21 Project for Medical Science, Yonsei University College of Medicine
[2]School of Electrical and Mechanical Engineering(Y.-C.R.), Yonsei University
This study was supported by BK21 Project for Medical Science and a faculty research grant of Yonsei University College of Medicine for 2001 (No. 2001 - 12).
Received July 22, 2003 ; Accepted September 15, 2003
Address reprint requests to : Tae-Sub Chung, M.D., Department of Diagnostic Radiology and Research Institute of Radiological Science, Yonsei University College of Medicine, YongDong Severance Hospital, 146-92 Dogok-dong, Kangnam-gu, Seoul 135-270, Korea.
Tel. 82-2-3497-3514 Fax. 82-2-3462-5472 E-mail: tschung@yumc.yonsei.ac.kr

The hemodynamic analysis of intracranial aneurysms is important not only in order to understand the pathophysiology of their growth and rupture (1-3), but also for their detection and the optimization of image quality at MRA (4). The enlargement and collapse of aneurysms is synchronized with the turnover volume of blood during each cardiac cycle. Their increasing volume during each cycle is identical to this turnover. The turnover volume can be an important factor not only in their hemodynamically caused growth and rupture, but also, due to the source of inflow, in the quality of the images obtained at noncontrast 3D-TOF MR angiography (MRA) and contrast-enhanced MR angiography (CEMRA).

The expansion and collapse of the elastic wall of real aneurysms is synchronized with the cardiac pulse; due to the absence of wall motion and a different inflow pattern, however, investigation using a hard-wall model suffers limitations (5).

The purpose of this study was to visualize turnover in terminal aneurysm phantoms of different neck sizes constructed using elastic silicon, and thus determine the extent to which compliance of the aneurysmal wall influences image quality at 3D-TOF MRA, CEMRA and DSA.

Materials and Methods

We designed home-made elastic silicon phantoms (Fig. 1) which mimicked basilar tip aneurysms (diameter of aneurysmal sac: 18 mm). *In-vitro* flow experiments were performed using phantoms of two different neck diameters (2 and 10 mm) connected to a computer-driven piston pump (UHDC, Ontario, Canada) programmed to pump forward at a systolic pumping volume of 30 (average, 9.196) ml per second. To maintain a viscosity similar to that of human blood, a solution of glycerine and distilled water (1.4:1) was used.

All 3D-TOF MRA and CEMRA studies involved the use of a 1.5-T MR system with a 25 mmT/m gradient capability (Siemens Vision, Erlangen, Germany). A 3D-TOF technique was used, with TR/TE of 30/6.4 msec, ramped pulses from 15 to 25 degrees, and a center flip angle of 20 degrees. A three-dimensional fast low-angle shot (3D-FLASH) MRA sequence was used for CEMRA; the imaging parameters were a repetition time of 3.2 msec, an echo time of 1.3 msec, a 35 °flip angle, an 80×160 matrix, a 175×280 mm field of view, and 7.18 seconds per sequence, with four phases. Ten mm of 50 mmol/L gadolinium chelate (gadopentate dimeglumine) (Magnevist; Schering, Berlin, Germany) was injected using a Spectris MR power injector (Medrad, U.S.A.) at a rate of 4 ml/sec via a side connector. Maximum intensity projection (MIP) images of each phase were evaluated to compare the difference between time taken for the main bolus to pass through the parent vessel and time to visualization of aneurysms by wash-in and out of contrast media.

For digital subtraction angiography (DSA) of the phantom, a Multistar T.O.P. (Siemens, Erlangen, Germany) was used, with a bolus injection of 4 ml of iodine contrast medium (Ultravist; Schering, Berlin, Germany) at a rate of 2 ml/sec via a connecting catheter and using an automatic infector. DSA images were obtained at rate of 6 frames/sec, and the pattern of circulation of the contrast bolus in the aneurysms and the flow pattern of the main bolus in the parent vessel were analyzed and compared with the findings of CEMRA and CFD studies.

Computational fluid dynamics (CFD) were used to analyze the flow patterns depicted at DSA and MR angiography, and the hemodynamics were thus expressed graphically.

CFD software (STAR-CD, CD-Adapco; UK and U.S.A., respectively) was used for this, and was run on a personal computer. The mesh was constructed by hand, and was based upon the X-ray images of the contrast-filled phantom. The flow pattern was described by vectors, according to direction and velocity, and the outflow boundary was set so as to have the same outflow volume in both branches.

The results were interpreted blindly by two radiologists (T-S.C., Y-J.L.) and one physicist (Y-C.R.), who reached a consensus. Results were compared and analyzed to validate that all results indicated a similar pattern of hemodynamics.

Fig. 1. Two elastic silicon phantoms were similar to basilar tip aneurysm (size of neck 10, 2 mm).

Results

3D-TOF MRA images relating to the broad-necked aneurysm phantom (10 mm) were better in terms of signal intensity and image quality than the narrow-necked phantom (Figs. 2B, 3B).

DSA images of the former demonstrated a larger volume of contrast media wash into aneurysms during the systolic phase, and faster washout (Fig. 2C). Images also showed, however, that during this phase, a small amount of contrast bolus gushed through the orifice of the narrow-necked aneurysm (2 mm) and moved to its dome, and that a smaller volume of contrast media washed into the aneurysms (Fig. 3C). DSA study showed that the turnover of narrow-necked aneurysms was less than that of broad-necked.

During CEMRA, the broad-necked aneurysm was visualized as the main bolus of Gd-DTPA passed through it. As the neck broadened, the volume of contrast bolus passing into the aneurysm increased (Figs. 2, 3). The narrow-necked aneurysm was visualized after passage of bolus Gd-DTPA and continuously visualized during delayed scanning (Fig. 3D). A signal intensity-time curve (Fig. 2E) showed that the signal intensity of the broad-necked aneurysm increased during the passage of contrast bolus through the parent vessel, but for the narrow-necked aneurysm, both the corresponding curve

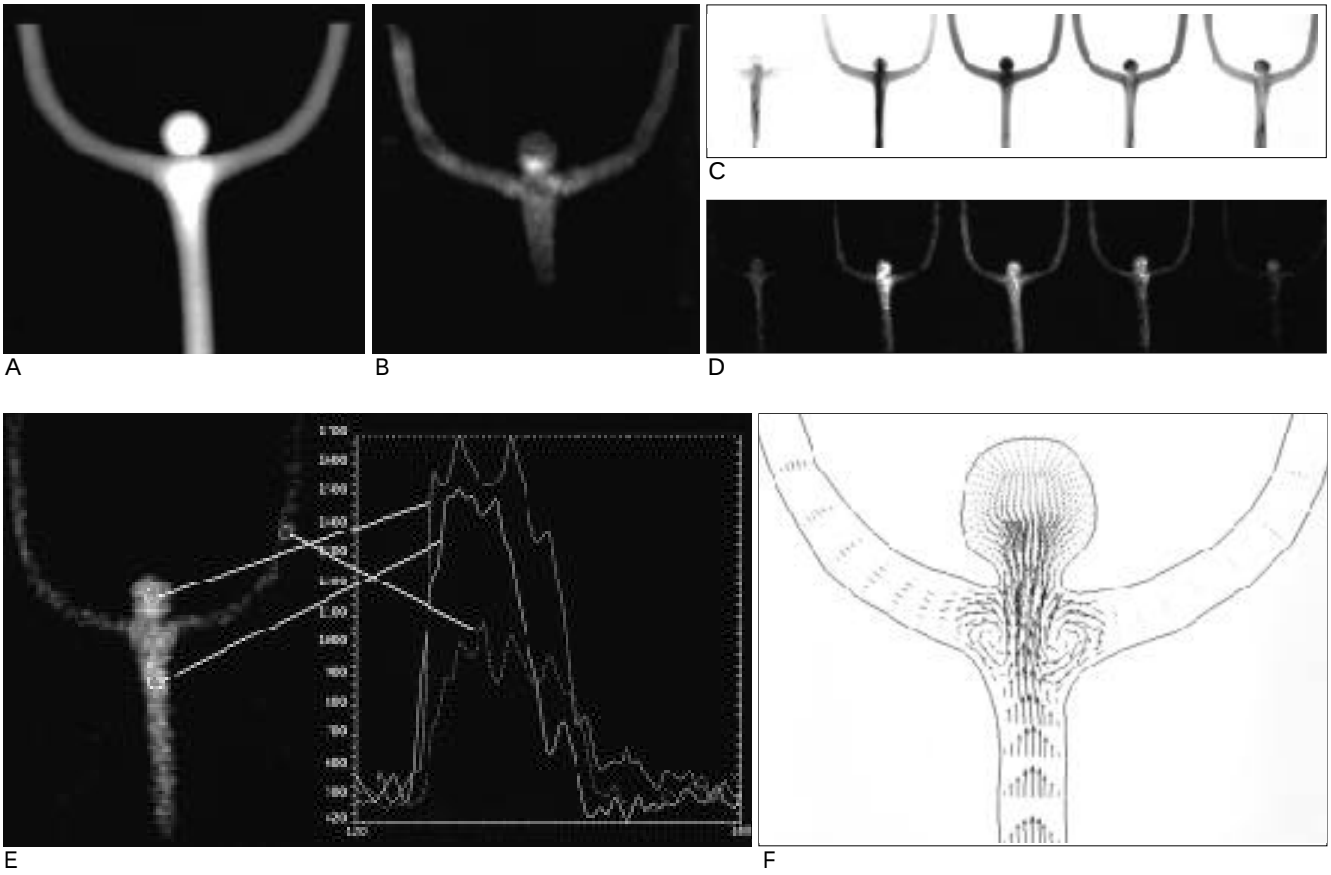

Fig. 2. Comparative evaluations on the phantom of broad-necked aneurysm.
A. Plain X-ray images of the broad neck (10 mm) of terminal saccular aneurysm phantoms were filled with contrast media (diameter of aneurysm sac:18 mm).
B. 3D-TOF MRA image showed good visualization of aneurysm sac.
C. The aneurysm sac was visualized with arrival of contrast media at parent vessel simultaneously on DSA study. Whole lumen of aneurysm was filled with contrast media on second systolic phase.
D. First phase of CEMRA showed simultaneous visualization of aneurysms sac with arrival of contrast media at parent vessel. Second phase of CEMRA showed more brightly visualized aneurysm lumen when the end of main bolus passed the parent vessel. Third phase of CEMRA revealed nonvisualization of aneurysm due to wash-out of contrast media from aneurysm sac with pass of contrast bolus.
E. Time-signal intensity curve of aneurysm shows fast turnover of contrast medium similar to parent vessel.
F. CFD reveals good inflow during systolic phase.

and the washout curve indicated delay (Fig. 3E).

Computational fluid dynamics (CFD) data for the systolic phase indicated substantial inflow gush into the broad-necked aneurysm (Fig. 2F), but weak jet stream inflow at the orifice of the narrow-necked aneurysm (Fig. 3F).

Discussion

Hemodynamically induced stress is an important factor affecting aneurysmal growth and rupture (1 - 3). Earlier investigations of both flow rate and flow pulsatility have made important contributions to the understanding of aneurysmal hemodynamics; non-contrast 3D-TOF MRA has depicted terminal saccular or broad-necked aneurysms, or both more clearly than lateral saccular or narrow-necked aneurysms, or both (4, 5). Aneurysmal blood turnover has also been presumed to have a significant effect on the signal intensity of aneurysms. Furthermore, the quality of CEMRA is greatly dependent upon the local concentration of contrast medium; to achieve optimal CEMRA, the bolus-injected medium must arrive at the carotid arteries in time to maintain an adequately high concentration (6). In this

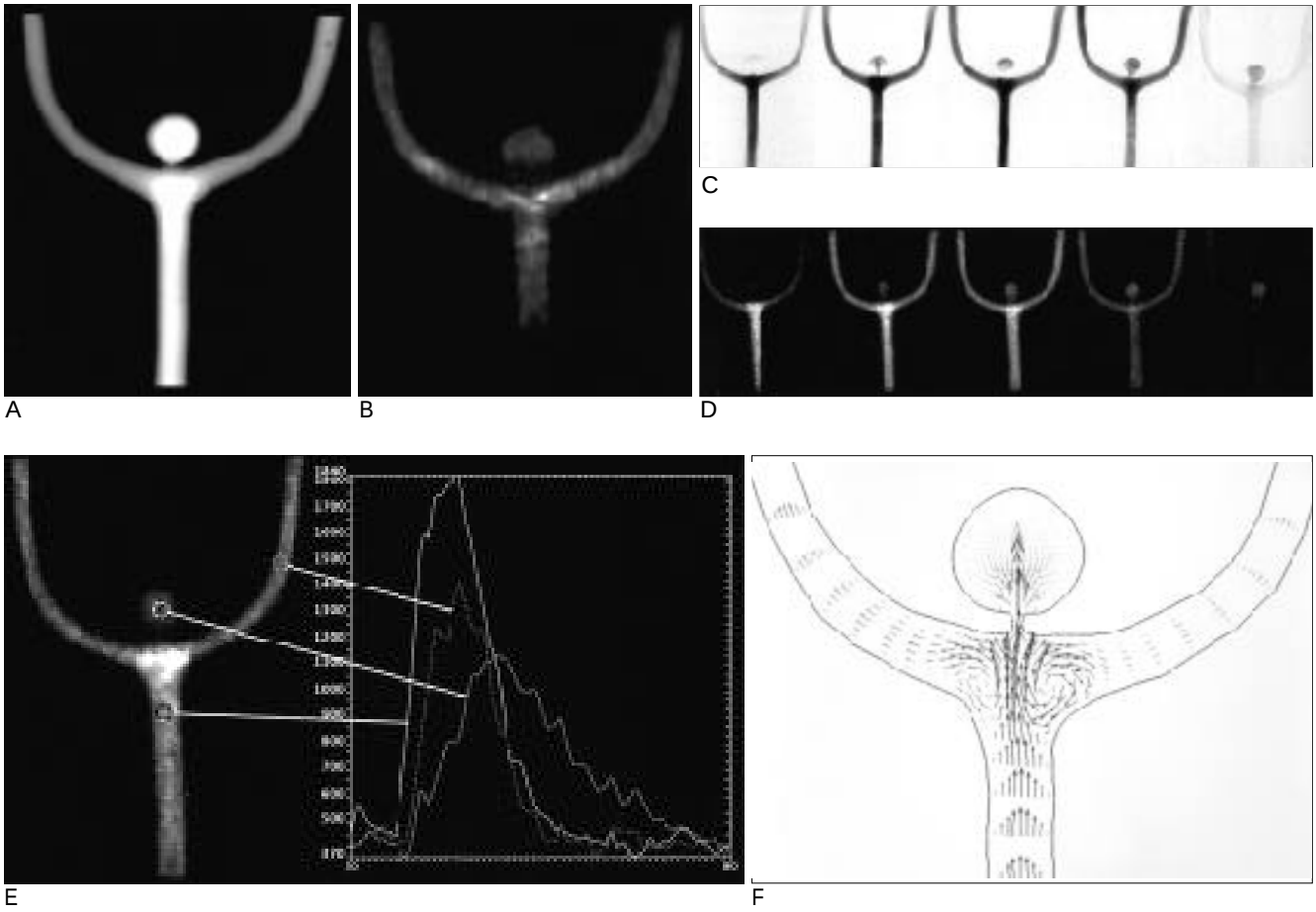

Fig. 3. Comparative evaluation on the phantom of narrow-necked aneurysm.
A. Plain X-ray images of the narrow neck (2 mm) of terminal saccular aneurysm phantoms filled with contrast media (diameter of aneurysm sac:18 mm).
B. 3D-TOF MRA image shows poor visualization of aneurysm sac.
C. Small fragment of contrast media entered into the phantom of aneurysm during the first systolic phase on DSA study. During second systolic phase, the first fragment of contrast media moved to the dome of aneurysm. Followed second fragment entered into the phantom of aneurysm. The gap between first and second fragment suggested discontinued wash-in during diastolic phase.
D. First phase of CEMRA showed very faintly visualized aneurysm lumen when the main bolus of contrast media arrived at parent vessel. Second phase of CEMRA showed more brightly visualized aneurysm lumen when the end of main bolus passed the parent vessel. Third phase of CEMRA showed delayed visualization of aneurysm after pass of main bolus.
E. Time-signal intensity curve of aneurysm shows delayed and diminished turnover of contrast medium.
F. CFD reveals small amount of inflow during systolic phase.

respect, recently developed high-resolution CEMRA allows 12 - 20 seconds for the evaluation of an intracranial aneurysm (7). Although some authors have emphasized that the center of k-space should coincide with the period of maximum effect during the first-pass bolus of contrast medium through arteries (7, 8), we insist that another important factor governing the optimal visualization of aneurysms at CEMRA is aneurysmal blood turnover when the bolus of contrast medium arrives at the aneurysms orifice.

Investigation of aneurysmal blood turnover is very important, not only to help provide an understanding of the mechanism of growth and rupture of aneurysms, but also for optimization of the imaging quality of noncontrast 3D-TOF MRA and CEMRA. Steiger et al. (9) emphasized that the most important determinant of intra-aneurysmal circulation was the geometrical relation between an aneurysm and its afferent vessel. Their experimental model, however, involved the use of hard walls, a choice which imposes certain limitations due to the rigidity (rather than compliance) of these walls during the cardiac cycle (5). To understand the hemodynamics of intracranial aneurysms, experiments involving the measurement of aneurysmal turnover and related wall compliance must consider factors such as the geometrical relation between aneurysms and their afferent vessel, their size, and the elasticity of the wall of the aneurysmal neck. Important studies of aneurysmal hemodynamics have included detailed analysis of flow dynamics in an aneurysm model (10), but CFD analyses can be accepted at face value for use in basic and comparative studies.

Our models were designed in the form of terminal aneurysms with elastic walls. Steiger et al. (9) showed that in hard-wall models, symmetric outflow led to flow stagnation in aneurysms and at their neck. In our experiments, even though the models of replicated symmetric terminal aneurysms, our results showed that turnover patterns were closely related to the elasticity of the aneurysmal wall and the size of their neck. Pulsatile flow studies have shown that segments of contrast bolus formed at the entrance to the aneurysm during each cardiac cycle (3); the extent of this formation could indicate the volume of aneurysmal turnover and degree of expansion during each cardiac cycle. In our experiments with elastic silicon phantoms of terminal aneurysms, flow was faster and turnover greater in the broad-necked aneurysm than in the narrow-necked. Furthermore, narrow-necked aneurysms were more likely to be missed, due to hemodynamic isolation, during DSA, 3D-TOF MRA and CEMRA. Aneurysmal blood turnover is an important factor in 1) the hemodynamic causes of aneurysmal growth and rupture, 2) the poor signal intensity of aneurysms during noncontrast 3D-TOF MRA, 3) their delayed or poor visualization during CEMRA, and 4) 3D rotational angiography (11).

Elastic silicon phantoms of aneurysms with pulsatile flow were an effective method for the evaluation of blood turnover in intracranial terminal aneurysms, a factor closely related to the size of the aneurysm's neck. Turnover during each cardiac cycle could be an important determinant not only of the hemodynamic causes of the growth and rupture of intracranial aneurysms, but also of the quality of non-contrast 3D-TOF MRA and CEMRA images used for their evalvation.

References

1. Tognetti F, Limoni P, Testa C. Aneurysm growth and hemodynamic stress. *Surg Neurol* 1983;20:74-78
2. Steiger HJ, Poll A, Liepsch DW, Reulen HJ. Haemodynamic stress in terminal aneurysms. *Acta Neurochir* 1988;93:18-23
3. Gobin YP, Counord JL, Flaud P, Duffaux J. In vitro study of haemodynamics in a giant saccular aneurysm model: influence of flow dynamics in the parent vessel and effects of coil embolisation. *Neuroradiology* 1994;36:530-536
4. Isoda H, Ramsey RG, Takehara Y, Takahashi M, Keneko M. MR angiography of aneurysma models of various shapes and neck sizes. *AJNR Am J Neuroradiol* 1997;18:1463-1472
5. Isoda H, Kinosada Y, Isogai S, Takehara Y, Ito T. Tagged MR imaging of intracranial aneurysm models. *AJNR Am J Neuroradiol* 1999;20:807-811
6. Lee YJ, Chung TS, Joo JY, Chien D, Laub G. Suboptimal contrast-enhanced carotid MR angiography from the left brachiocephalic venous stasis. *J Magn Reson Imaging* 1999;10:503-509
7. Isoda H, Takehara Y, Isogai S, et al. Software-triggered contrast-enhanced three-dimensional MR angiography of the intracranial arteries. *AJR Am J Reontgenol* 2000;174:371-375
8. Maki JH, Prince MR, Londy FJ, Chenevert TL. The effects of time varying intravascular signal intensity and K-space acquisition order on three-dimensional MR angiography image quality. *J Magn Reson Imaging* 1996;6:642-651
9. Steiger HJ, Poll A, Liepsch DW, Reulen HJ. Basic flow structure in saccular aneurysms: a flow visualization study. *Heart Vessels* 1987;3:55-65
10. Steinman DA, Milner JS, Norley CJ, Lownie SP, Holdsworth DW. Image-based computational simulation of flow dynamics in a giant intracranial aneurysm. *AJNR Am J Neuroradiol* 2003;24:559-566
11. Ernemann UU, Gronewaller E, Duffner FB, Guervit O, Claassen J, Skalej MD. Influence of geometric and hemodynamic parameters on aneurysmas visualization during three-dimensional rotational angiography: an in vitro study. *AJNR Am J Neuroradiol* 2003;24: 597-603

대한방사선의학회지 2003;49:387-392

두개강내 동맥류모형의 혈액순환: 경부직경과의 연관성[1]

[1]연세대학교의과대학진단방사선과학교실
[2]연세대학교공과대학기계공학부

정태섭 · 이영준 · 임윤철[2]

목적: 삼차원유체속도강조 자기공명혈관조영술(3D-TOF MRA), 조영증강 자기공명혈관조영술(CEMRA)과 디지털 감산 혈관조영술(DSA)때 혈류역학적 격리현상으로 인해 동맥류가 잘 보이지 않는 생리학적 배경을 실험연구로 밝히고자한다.

대상과방법: 비교연구를위한수제품의탄성형실리콘말단형동맥류모형내의혈액순환을연구하였다. 기저동맥동맥류와유사한모양의 2, 10 mm 경부직경을 가진두가지의탄성형동맥류 모형에 인체 조건과 유사한박동성펌프를 부착한 후 3D-TOF MRA, CEMRA와 DSA를 시행하며 혈류역학적 실험을 하였다. 각각의 결과는 전산유체역학 결과와 비교하였다.

결과: DSA실험에서 좁은경부직경을가진동맥류모형에서는심수축기동안소량의 조영제가동맥류내로 순환유입되었다. 동맥류 경부의 직경이 넓어지며 순환유입되는 조영제의 양도 점차 많아졌다. 넓은 경부 직경을 가진 동맥류모형에서는 CEMRA때 조영제가 동맥부위를 지나갈 때 동시에 동맥류가 보였다. 그러나 2 mm의 좁은 경부직경을 가진 동맥류모형에서는 CEMRA때 동맥부위를 조영제가 지나간 후 지연CEMRA에서 동맥류가 희미하게 보였다. 이들 결과는 3D-TOF MRA와전산유체역학결과와잘일치하였다.

결론: 3D-TOF MRA, CEMRA와 DSA에서 두개강내동맥류의 표현은 동맥류 경부의크기에따른혈액순환에 크게 영향을 받으므로 경부직경이 좁은 동맥류는 혈류역학적 격리현상으로 인해 방사선학적 검사때 발견하지 못 할 가능성이 있다.